

Tennessee State University

## Digital Scholarship @ Tennessee State University

---

Information Systems and Engineering  
Management Research Publications

Center of Excellence in Information Systems  
and Engineering Management

---

11-1998

### A Search for Lithium-rich Giants among Stars with Infrared Excesses

Francis C. Fekel  
*Tennessee State University*

Lyndon C. Watson  
*University of Canterbury*

Follow this and additional works at: <https://digitalscholarship.tnstate.edu/coe-research>



Part of the [Stars, Interstellar Medium and the Galaxy Commons](#)

---

#### Recommended Citation

Francis C. Fekel and Lyndon C. Watson 1998 AJ 116 2466

This Article is brought to you for free and open access by the Center of Excellence in Information Systems and Engineering Management at Digital Scholarship @ Tennessee State University. It has been accepted for inclusion in Information Systems and Engineering Management Research Publications by an authorized administrator of Digital Scholarship @ Tennessee State University. For more information, please contact [XGE@Tnstate.edu](mailto:XGE@Tnstate.edu).

## A SEARCH FOR LITHIUM-RICH GIANTS AMONG STARS WITH INFRARED EXCESSES

FRANCIS C. FEKEL<sup>1</sup>

Center for Automated Space Science and Center of Excellence in Information Systems, Tennessee State University, 330 10th Avenue North, Nashville, TN 37203; fekel@coe.tnstate.edu

AND

LYNDON C. WATSON

Mount John University Observatory and Department of Physics and Astronomy, University of Canterbury, Private Bag 4800, Christchurch, New Zealand; l.watson@csc.canterbury.ac.nz

Received 1998 June 18; revised 1998 August 6

### ABSTRACT

The unusual nature of the single, rapidly rotating, lithium-rich K giant HDE 233517, which is currently undergoing significant mass loss, prompted a search for giants with similar properties. High-dispersion spectroscopic observations were obtained of HD 219025, a known lithium-rich infrared-excess giant, plus 39 stars from a list of G and K giants with excess far-infrared emission. The projected rotational velocities of the vast majority of infrared-excess giants appear to be similar to those of normal G and K giants. Six giants have lithium abundances at or above theoretical upper envelope values. The percentage of such stars in the sample of 39 infrared-excess giants is similar to that of normal giants. The three giants with the largest lithium abundances have previously been discovered. None of the sample of 39 giants have an H $\alpha$  line similar to the broadened and very asymmetric line of HDE 233517. The star with optical properties most similar to HDE 233517 is HD 219025.

*Key words:* stars: abundances — stars: peculiar

### 1. INTRODUCTION

Over the past few years, searches for late-type stars with infrared excesses have been carried out for various reasons. Zuckerman, Kim, & Liu (1995) examined the *IRAS* catalogs for giants having associated dust and presented a conservative list of 92 stars. Plets et al. (1997) conducted a similar search for late-type giants with far-infrared excesses. Both groups found that a small fraction of late-type giants are surrounded by extensive dust, concluded that the stars are likely first-ascent giants, and examined possible explanations for the occurrence of the dust.

The *IRAS* catalogs have also provided fertile ground for the discovery of individual stars with specific properties. To identify new T Tauri stars, Gregorio-Hetem et al. (1992) obtained spectroscopic and photometric observations of about 100 stars chosen according to their *IRAS* colors. As a by-product of that search, they identified four lithium-rich giants. Gregorio-Hetem, Castilho, & Barbuy (1993) showed that in an infrared color-color diagram giants with low lithium abundances were segregated from lithium-rich giants. Those findings resulted in an extensive ongoing search for additional lithium-rich giants, based on their *IRAS* colors. Castilho et al. (1998) have presented a status report on that survey. De la Reza, Drake, & da Silva (1996) proposed a scenario relating lithium abundances and infrared excesses in late-type giants. De la Reza et al. (1997) expanded their observational sample by observing 27 of the giants in the list of Zuckerman et al. (1995) and including other stars from the literature.

A decade ago, Walker & Wolstencroft (1988) compiled a short finding list of objects with infrared characteristics similar to Vega,  $\beta$  Pic, and  $\epsilon$  Eri, which included the unusual

late-type stars HD 98800 and HDE 233517. Skinner et al. (1995) argued that HDE 233517 is a young, chromospherically active K dwarf similar to HD 98800. However, Fekel et al. (1996) obtained high-dispersion spectroscopic observations that led them to the conclusion that HDE 233517 is not a dwarf but a very unusual K giant. They classified the spectrum as K2 III and noted other characteristics that supported the giant classification. While no velocity variations were found, implying that the star is single, it has significant line broadening,  $v \sin i = 15 \text{ km s}^{-1}$ . Along with its rapid rotation, Fekel et al. (1996) reported that HDE 233517 has modest Ca II H and K emission and a very large lithium abundance of  $\log \epsilon(\text{Li}) \sim 3.3$ . Such characteristics are similar to a group of chromospherically active single giants discussed by Fekel & Balachandran (1993). However, the shape of the H $\alpha$  line of HDE 233517 is distinctly different, being reminiscent of line profiles seen in supergiants, and implies that the star is undergoing significant mass loss (Fekel et al. 1996). Fekel et al. (1996) also discussed the star HD 219025, whose known properties appeared to be similar to those of HDE 233517.

The present search was initiated to determine whether other infrared-excess giants have properties similar to HDE 233517 and the single giants discussed by Fekel & Balachandran (1993). To that end, spectroscopic observations were obtained of several different wavelength regions, including those of lithium and H $\alpha$ , for a sample of 39 infrared-excess giants plus HD 219025.

### 2. OBSERVATIONS

From the list of Zuckerman et al. (1995), a subset of 39 stars brighter than  $V = 10.0$  mag and north of  $-40^\circ$  was observed. From 1996 April through 1998 April, high-dispersion spectroscopic observations were obtained at Kitt Peak National Observatory with the coudé feed telescope, coudé spectrograph, and a TI CCD detector. Nearly all the stars were observed at both the lithium and H $\alpha$

<sup>1</sup> Visiting Astronomer, Kitt Peak National Observatory, National Optical Astronomy Observatories, operated by the Association of Universities for Research in Astronomy, Inc., under cooperative agreement with the National Science Foundation.

wavelengths. Fourteen of the stars have at least one additional observation centered at a wavelength of 6430 Å. Observations of those three wavelength regions have a wavelength range of about 80 Å and a resolution of 0.21 Å.

Bias subtraction, flat-field division, wavelength calibration, and continuum rectification were performed on the raw spectra with the programs in IRAF (distributed by NOAO). The thorium-argon comparison spectra were obtained at intervals of 1–2 hr. The wavelength solution for a spectrum was applied by interpolating in time between the two comparison spectra that bracketed the stellar spectrum.

The southern star HD 219025 was observed at the Mount John University Observatory (MJUO), Lake Tekapo, New Zealand, on two nights in 1995 August. High-dispersion spectra centered on 6612 Å were obtained with the 1 m McLellan Telescope (Nankivell & Rumsey 1986), the MJUO echelle spectrograph (Hearnshaw 1977, 1978), and a Thompson CCD detector. The 6708 Å lithium line was observed in order 34 of the spectrograph, for which the dispersion is 1.22 Å mm<sup>-1</sup> and the resolving power  $R = 40,000$ . Portions of three other orders also fell on the CCD, the most useful of which was order 36, centered on 6330 Å.

The spectra of HD 219025 were reduced at the University of Canterbury with the Munich Image Data Analysis (MIDAS) software supplied by the Image Processing Group of the European Southern Observatory. With standard MIDAS procedures, dispersion solutions were computed from thorium-argon spectra obtained immediately after each stellar spectrum. The spectra were median filtered to reduce cosmic-ray strikes but were not otherwise smoothed.

### 3. BASIC PROPERTIES

The basic properties of the 39 program stars plus HD 219025 are listed in Table 1. Columns (1)–(3) list the HD number, the HR number, and *Hipparcos* catalog number, respectively. The spectral types of the stars are given in column (4). Aside from our new classifications, they come primarily from Houk (Houk 1982; Houk & Smith-Moore 1988), Roman (1952), and Keenan & McNeil (1989). Only as a last resort was an unreferenced spectral type assumed from the Bright Star Catalogue (preliminary 5th ed.; D. Hoffleit & W. H. Warren 1993, private communication). Column (5) gives the  $V$  magnitude, and column (6) gives the  $B - V$  color of each star. The magnitudes and colors are primarily from the Bright Star Catalogue (preliminary

TABLE 1  
INFRARED-EXCESS GIANTS

HD (1)	HR (2)	HIP (3)	Spectral Type (4)	$V$ (mag) (5)	$B - V$ (mag) (6)	$\pi$ (arcsec) (7)	$v \sin i$ (km s <sup>-1</sup> ) (8)
6	2	417	G9 III	6.29	1.10	0.00695	2.8
3627	165	3092	K3 III	3.27	1.28	0.03219	2.6
21078	...	15769	K0 III/IV	8.00	0.92	0.01182	2.2
27497	1360	20268	G8 III <sup>a</sup>	5.77	0.92	0.00762	3.1
30834	1551	22678	K3 III <sup>a</sup>	4.78	1.41	0.00581	2.7
31553	1586	23068	K1 III <sup>a</sup>	5.79	1.11	0.00692	2.7
34043	1709	24450	K4 III	5.50	1.37	0.00545	3.4
39806	...	27811	K3 III	8.39	1.45	0.00275	3.2
40359	2098	28138	G8 III	6.44	1.07	0.00420	4.6
43827	2260	29895	K3 III	5.14	1.30	0.00575	3.0
49628	...	...	G8 III	8.2	...	...	2.0
69530	...	40552	K3 III	7.17	1.48	0.00198	3.1
80989	...	...	K1/K2 III	9.0	...	...	3.0
94363	4249	53240	G9 III <sup>a</sup>	6.12	0.90	0.01251	1.8
114182	...	...	G6 III	9.7	...	...	2.7
119853	5173	67172	G8 III <sup>a</sup>	5.51	0.90	0.00860	2.6
129456	5485	72010	K3 III <sup>a</sup>	4.05	1.35	0.01589	3.7
131530	5554	72934	K0 III <sup>a</sup>	5.80	0.97	0.00894	2.1
138688	5775	76259	K3 III <sup>a</sup>	5.15	1.30	0.00884	3.1
139997	5838	76880	K5 III	4.74	1.57	0.00816	4.2
143619	5965	78575	K3 III	6.03	1.31	0.00723	3.3
145206	6016	79195	K4 III	5.37	1.45	0.00660	3.2
146850	6078	79938	K3 III <sup>a</sup>	5.94	1.52	0.00377	3.5
153135	...	83045	K3 III <sup>a</sup>	7.16	1.56	0.00841	3.0
153194	...	...	K0 III	8.6	...	...	2.9
153687	6318	83262	K5 III <sup>a</sup>	4.82	1.48	0.00811	4.5
156061	...	84494	K1 III <sup>a</sup>	7.14	1.18	0.00614	1.9
156115	...	84481	K5 III	6.59	1.79	0.00392	3.4
169689	6902	90313	G9 II + B8 V	5.65	0.92	0.00404	9.5
170659	...	90811	K5/M0 III	8.50	1.76	0.00218	5.3:
175492	7133	...	G7 III + A <sup>a</sup>	4.59	0.78	...	4.9
181154	...	95040	K0 III	8.37	1.19	0.00659	2.8
190299	7667	98844	K4 III	5.68	1.30	0.00560	2.0
202320	8127	104963	K0 II/III	5.24	1.17	0.00472	3.8
204082	...	105930	K4 III	8.00	1.47	0.00021	2.0
204540	...	106036	K2 III	6.55	1.29	0.00333	4.0
212320	8530	110532	G6 III	5.93	1.00	0.00710	4.8
218527	8807	114273	G7 III <sup>a</sup>	5.40	0.91	0.01164	2.9
219025	...	114678	K2 IIIp	7.67	1.21	0.00325	...
221776	8950	116365	K7 III	6.18	1.58	0.00481	4.4

<sup>a</sup> Spectral type classified in this paper.

TABLE 2  
RADIAL VELOCITIES OF INFRARED-EXCESS GIANTS

HD (1)	HR (2)	HJD - 2,400,000 (3)	Radial Velocity (km s <sup>-1</sup> ) (4)	Wavelength (Å) (5)	Comment (6)
6	2	50,400.670	15.0	6707	
		50,404.635	14.9	6565	
3627	165	50,400.674	-10.7	6707	
		50,404.654	-10.6	6565	
21078	...	50,400.803	27.4	6707	Variable
		50,831.710	53.4	6565	
27497	1360	50,400.817	5.9	6707	Variable
		50,831.788	2.4	6565	
		50,832.741	2.5	6430	
30834	1551	48,578.755	-17.1	6430	
		50,400.827	-16.7	6707	
		50,831.698	-17.6	6565	
		50,831.805	-17.2	6565	
31553	1586	50,400.831	-4.2	6707	
		50,831.799	-3.4	6565	
		50,832.748	-3.6	6430	
34043	1709	50,400.834	-3.1	6707	
		50,831.794	-2.6	6565	
39806	...	50,400.915	46.4	6707	
		50,831.733	46.4	6565	
40359	2098	50,400.935	27.3	6707	
		50,831.748	26.9	6565	
43827	2260	50,400.942	-8.2	6707	
		50,831.754	-8.5	6565	
49628	...	50,400.977	19.1	6707	Variable
		50,831.768	11.8	6565	
69530	...	50,401.014	-7.4	6707	
		50,831.820	-8.2	6565	
80989	...	50,401.026	36.4	6707	
		50,831.852	36.2	6565	
94363	4249	50,577.770	21.5	6430	Known variable
		50,633.641	20.6	6707	
		50,831.877	19.8	6565	
114182	...	50,633.670	-11.9	6707	
119853	5173	50,200.855	-10.2	6565	Variable?
		50,577.780	-8.7	6430	
		50,633.638	-8.7	6707	
		50,927.865	-8.7	6430	
129456	5485	50,200.858	-38.9	6565	
		50,633.635	-38.1	6707	
		50,927.870	-38.7	6430	
131530	5554	50,200.869	-20.3	6565	
		50,576.879	-19.7	6707	
		50,632.714	-19.6	6430	
138688	5775	50,200.861	23.9	6565	Known variable
		50,576.874	7.7	6707	
		50,927.874	11.6	6430	
139997	5838	50,200.864	-3.0	6565	Known variable
		50,576.883	-10.9	6707	
143619	5965	50,200.872	3.4	6565	
		50,576.887	4.1	6707	
145206	6016	50,200.877	-53.5	6565	Known variable
		50,576.929	-51.9	6707	
146850	6078	50,200.890	-26.6	6565	Variable
		50,576.924	-28.0	6707	
		50,632.721	-28.1	6430	
		50,927.921	-29.6	6430	
153135	...	50,200.882	-26.7	6565	
		50,576.917	-26.0	6707	
		50,928.947	-25.4	6430	
153194	...	50,200.902	-47.5	6565	
		50,576.901	-47.1	6707	
153687	6318	50,200.914	-7.9	6565	
		50,576.950	-7.4	6707	
		50,928.958	-7.8	6430	
156061	...	50,200.921	53.5	6565	
		50,576.935	54.3	6707	
		50,632.774	54.5	6430	
156115	...	50,200.933	-9.6	6565	
		50,576.946	-10.1	6707	
169689	6902	50,200.940	-6.0	6565	Known variable
		50,576.976	-6.2	6707	

TABLE 2—Continued

HD (1)	HR (2)	HJD – 2,400,000 (3)	Radial Velocity (km s <sup>-1</sup> ) (4)	Wavelength (Å) (5)	Comment (6)
170659.....	...	50,576.966	3.7	6707	
175492.....	7133	50,200.941	–35.2	6565	Known variable
		50,632.003	–13.3	6430	
181154.....	...	50,400.574	17.0	6707	
		50,404.569	16.9	6565	
190299.....	7667	50,200.947	1.1	6565	
		50,400.605	1.8	6707	
202320.....	8127	50,200.961	–5.1	6565	
		50,400.627	–4.2	6707	
204082.....	...	50,400.617	38.9	6707	
		50,404.589	38.9	6565	
204540.....	...	50,200.965	–24.3	6565	
		50,400.652	–23.7	6707	
212320.....	8530	50,201.000	–8.2	6565	
		50,400.646	–7.2	6707	
218527.....	8807	50,201.010	–15.0	6565	Variable
		50,400.659	–7.5	6707	
		50,633.948	–25.9	6430	
		50,637.864	–25.5	6430	
		50,831.615	–37.2	6430	
219025.....	...	49,942.893	–26.1	6330	
		49,943.861	–26.7	6330	
221776.....	8950	50,201.003	–13.5	6565	
		50,400.664	–13.8	6707	

5th ed.; D. Hoffleit & W. H. Warren 1993, private communication) or The Hipparcos and Tycho Catalogues (ESA 1997). The *Hipparcos* parallaxes (ESA 1997) are listed in column (7), while the projected rotational velocities, determined from our KPNO observations, are listed in column (8).

From the spectra, spectral types and radial velocities were determined for the KPNO program stars. Those analyses and measurements are briefly described below.

Spectral types were determined by visual comparison for those stars with spectra covering the 6430 Å region. Spectral type standards were observed from the list of Keenan & McNeil (1989). Strassmeier & Fekel (1990) identified several luminosity-sensitive and temperature-sensitive line ratios in the 6430–6465 Å region. Those critical line ratios and the general appearance of the spectrum were used as spectral type criteria. The new spectral types are given in Table 1.

Radial velocities of the KPNO program stars were determined with the IRAF cross-correlation program FXCOR (Fitzpatrick 1993). Radial velocities for IAU standard stars were assumed from Scarfe, Batten, & Fletcher (1990). For the H $\alpha$ -region spectra, the H $\alpha$  line was excluded from velocity measurement, and only the region redward of that line was measured. In Table 2 the stars are identified by HD and HR numbers in columns (1) and (2), respectively. Column (3) lists the Heliocentric Julian Date, and column (4), the measured radial velocity. The velocities have typical uncertainties of  $\leq 0.5$  km s<sup>-1</sup>. Column (5) identifies the wavelength region observed. Brief comments on the velocity variability of some of the stars are given in column (6).

Radial velocities of HD 219025 were determined by fitting individual lines with Gaussians to determine their observed wavelengths. The rest wavelengths of the four Fe I lines used were 6322.694, 6335.337, 6336.830, and 6703.576 Å. The wavelength differences were converted to a velocity difference and corrected for Earth's motion. The velocities have uncertainties of 2–3 km s<sup>-1</sup>.

#### 4. PROJECTED ROTATIONAL VELOCITIES

Rotational velocities were determined from the KPNO red-wavelength spectra with the procedure of Fekel (1997). The FWHM of about a half-dozen weak or moderate-strength lines was measured, and the results averaged. An instrumental broadening of 0.21 Å was removed from the measured mean broadening by taking the square root of the difference of the squares of the two measurements, resulting in the intrinsic stellar broadening. Next, the calibration polynomial of Fekel (1997) was used to convert this broadening in angstroms into a total line broadening in km s<sup>-1</sup>. Finally, the macroturbulence was removed by taking the square root of the difference of the squares, resulting in the projected rotational velocity. As in Fekel (1997), a macroturbulence of 4 km s<sup>-1</sup> was assumed for mid-G giants and a value of 3 km s<sup>-1</sup> was assumed for late G and K giants. For the bright giants HR 6902 and HR 8127, a value of 5 km s<sup>-1</sup> was used, while 2 km s<sup>-1</sup> was used for the subgiant HD 21078. The projected rotational velocities listed in Table 1 have uncertainties of 0.5–1 km s<sup>-1</sup>. Uncertainties are greatest for those stars having rotational velocities less than 3 km s<sup>-1</sup> since their line widths are dominated by macroturbulence rather than rotation.

Gray (1989) and de Medeiros & Mayor (1990) showed that the vast majority of G and K giants are slowly rotating. From the projected rotational velocities of 1100 bright giants in the spectral range F5–K5, de Medeiros, da Rocha, & Mayor (1996) found mean rotational velocities of 3.3 km s<sup>-1</sup> for mid-G giants and 2.2 km s<sup>-1</sup> or less for late G and K giants. De Medeiros, Melo, & Mayor (1996) determined the rotational velocities for a dozen lithium-rich giants. From that sample they concluded that even the most lithium-rich giants have rotational velocities similar to normal giants. Thus, the large projected rotational velocity of HDE 233517 and other chromospherically active *single* giants (Fekel & Balachandran 1993) is quite unusual and, therefore, an identification hallmark.

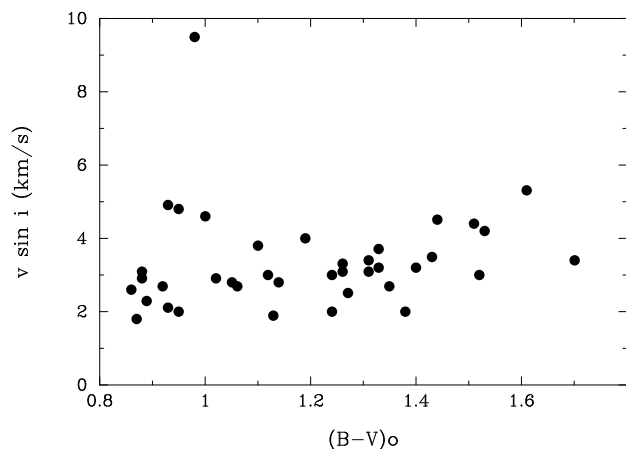


FIG. 1.—Projected rotational velocities of 39 G and K giants vs.  $(B-V)_0$ .

Rotational velocities of 39 giants, whose spectra were obtained at KPNO, are plotted versus  $(B-V)_0$  in Figure 1. Only one star, HR 6902, has a large rotational velocity. That star is a bright giant and a composite spectrum binary. Excluding HR 6902, the mean rotational velocity of the sample is  $3.2 \text{ km s}^{-1}$ . The seven stars with  $(B-V)_0 > 1.40$ , which corresponds to a spectral type of K4 III or later, have a mean  $v \sin i = 4.0 \text{ km s}^{-1}$ . The increased mean rotational velocity for the coolest stars is likely the result of a lack of weak unblended lines available for measurement in the observed spectral regions. Thus, most if not all of those values are probably upper limits. With that group also excluded, the remaining sample of 31 stars has a mean of  $3.0 \text{ km s}^{-1}$ .

## 5. LITHIUM ABUNDANCES

For the KPNO observations the lithium line was fitted with a Gaussian profile to determine its equivalent width. However, at a resolution of  $0.21 \text{ \AA}$ , the blue side of the lithium line is blended with the Fe I line at  $6707.44 \text{ \AA}$ . For the coolest program stars, the red side of the lithium line is also significantly blended. Thus, two and sometimes three Gaussian profiles were needed to deblend the observed lithium feature. In some spectra the lithium line appears to be absent or nearly absent. A minimum value of  $4 \text{ m\AA}$  for the lithium equivalent width was estimated from the fit to other weak lines near the lithium wavelength.

The lithium equivalent width of HD 219025 was measured using a single Gaussian profile as well as with a triangle approximation. We obtained a mean lithium equivalent width of  $456 \text{ m\AA}$ . Such an equivalent width is similar to the value of  $430 \text{ m\AA}$  found by Pallavicini, Randich, & Giampapa (1992) for the Li I + Fe I blend. Using an effective temperature of  $4060 \text{ K}$ , Randich, Gratton, & Pallavicini (1993) determined  $\log \epsilon(\text{Li}) = 2.2$ . However, a substantially higher effective temperature for HD 219025, which would result in a significantly larger lithium abundance, is indicated by its spectral type and  $(B-V)_0 = 1.11$ .

To convert an equivalent width to a lithium abundance, an effective temperature was determined. The observed  $B-V$  was converted to  $(B-V)_0$ , assuming  $E(B-V) = A_V/3$  and  $A_V = 1 \text{ mag kpc}^{-1}$ . Then the temperature was assumed from the  $(B-V)$ -effective temperature relation of Flower

(1996). For those few stars without an observed  $B-V$ , the effective temperature was assumed from the spectral type- $(B-V)$  relation of Gray (1992). Finally, Table 2 of Soderblom et al. (1993) was used to determine a lithium abundance. Although that table was computed for dwarfs, the lithium abundance is primarily dependent on the assumed effective temperature and much less so on gravity (e.g., Brown et al. 1989; Pallavicini, Cerruti-Sola, & Duncan 1987). The uncertainties in the logarithmic abundances are estimated to be  $\pm 0.4$ .

The lithium results are given in Table 3. Columns (1) and (2) identify the stars by HD and HR numbers, respectively. Column (3) lists the computed  $(B-V)_0$  value, and column (4), the associated effective temperature. Column (5) gives the measured lithium equivalent width, and column (6), the computed log lithium abundance. Columns (7)–(9) list measurements of the  $H\alpha$  line and are discussed in § 6.

As a result of convective dilution, a red giant is theoretically expected to have a lithium abundance of  $\log \epsilon(\text{Li}) < 1.5$  (Iben 1967a, 1967b). Over the past decade, a modest but growing number of lithium-rich late-type giants have been found. The most extensive survey to date is that of Brown et al. (1989), who observed 644 stars to assess the frequency of apparently normal G–K giants with anomalously high lithium abundances. Less than 1.5% of their sample have  $\log \epsilon(\text{Li}) \geq 1.8$ , only 4% have  $\log \epsilon(\text{Li}) \geq 1.3$ , and an additional 4% have abundances between 1.2 and 1.3. Thus, even the upper envelope of the theoretically predicted upper limit is rarely occupied.

Out of the KPNO sample of 39 stars, two stars have lithium equivalent widths of over  $300 \text{ m\AA}$ . The large lithium abundances of those two stars, HD 30834 (Brown et al. 1989) and HD 146850 (Castilho, Barbuy, & Gregorio-Hetem 1995), have previously been discovered. Three other stars, HD 21078, HR 2098, and HR 5554, have  $\log \epsilon(\text{Li}) = 1.3$ . Thus, in this modest-sized sample of infrared-excess giants, the percentage of giants with  $\log \epsilon(\text{Li}) \geq 1.2$  is similar to that expected for normal field giants (Brown et al. 1989), 13% versus 8%.

De la Reza et al. (1997) observed 27 late-type giants from the list of Zuckerman et al. (1995) but discovered no new “Li K giants.” However, de la Reza et al. (1997) did not actually determine lithium abundances for those stars but defined a “Li K giant” as a giant with a Li I  $\lambda 6708$  line of comparable intensity to the Ca I  $\lambda 6717$  line. For giants with known lithium abundances, they defined a “Li K giant” as a giant with a lithium abundance higher than  $\log \epsilon(\text{Li}) = 1.2$ . Ten of the giants in the present study are in common with that study. The only slightly discrepant result is for HR 5554, which has  $\log \epsilon(\text{Li}) = 1.3$  in the present study and, thus, would just qualify as a “Li K giant.”

## 6. $H\alpha$ RESULTS

Three quantities were measured to characterize the  $H\alpha$  line: the reciprocal central intensity,  $R_c$ ; the full width at half-depth, FWHD; and the core equivalent width,  $EW_c$ . The core equivalent width was determined in a manner similar to that described by Bopp, Dempsey, & Maniak (1988) and Strassmeier et al. (1990). Such core equivalent widths also were measured by Eaton (1995) in his extensive atlas of  $H\alpha$  spectra. The sides of the line core are extended to the continuum, and the equivalent width of that area is measured. Such a measurement eliminates most of the nearby water vapor lines and uncertainties in equivalent

TABLE 3  
LITHIUM ABUNDANCES AND H $\alpha$  MEASUREMENTS OF INFRARED-EXCESS GIANTS

HD (1)	HR (2)	( $B-V$ ) <sub>0</sub> <sup>a</sup> (mag) (3)	$T_{\text{eff}}$ (K) (4)	EW (mÅ) (5)	log $\epsilon(\text{Li})$ (6)	$R_c$ (7)	FWHD (Å) (8)	EW <sub>c</sub> (Å) (9)
6	2	1.05	4748	5	0.1	0.186	1.32	1.07
3627	165	1.27	4366	11	-0.1	0.203	1.29	1.01
21078	...	0.89	5068	33	1.3	0.200	1.27	1.02
27497	1360	0.88	5090	5	0.5	0.180	1.34	1.11
30834	1551	1.35	4234	375	2.5	0.188	1.48	1.18
31553	1586	1.06	4731	15	0.5	0.213	1.39	1.10
34043	1709	1.31	4300	≤4	≤-0.7	0.182	1.36	1.11
39806	...	1.33	4266	5	0.6	0.171	1.45	1.17
40359	2098	1.00	4843	54	1.3	0.185	1.45	1.18
43827	2260	1.24	4415	8	-0.2	0.175	1.42	1.14
49628	...	0.95 <sup>b</sup>	4943	≤4	≤0.2	0.177	1.32	1.11
69530	...	1.31	4300	44	0.4	0.158	1.42	1.17
80989	...	1.12 <sup>b</sup>	4614	8	0.1	0.189	1.31	1.04
94363	4249	0.87	5114	≤4	≤0.4	0.208	1.45	1.17
114182	...	0.92 <sup>b</sup>	5004	18	1.0	...	...	...
119853	5173	0.86	5136	≤4	≤0.4	0.189	1.36	1.14
129456	5485	1.33	4266	7	-0.5	0.185	1.38	1.12
131530	5554	0.93	4984	36	1.3	0.189	1.34	1.10
138688	5775	1.26	4382	18	0.1	0.197	1.37	1.11
139997	5838	1.53	3926	≤7	≤-0.7	0.180	1.42	1.16
143619	5965	1.26	4382	≤4	≤-0.6	0.188	1.33	1.08
145206	6016	1.40	4153	90	0.6	0.195	1.34	1.08
146850	6078	1.43	4103	315	2.1	0.188	1.56	1.28
153135	...	1.52	3945	≤4	≤-1.0	0.191	1.33	1.07
153194	...	1.02 <sup>b</sup>	4815	≤4	≤0.1	0.188	1.31	1.06
153687	6318	1.44	4086	47	0.2	0.194	1.38	1.08
156061	...	1.13	4605	41	0.8	0.184	1.34	1.10
156115	...	1.70	3457	≤4	≤-1.0	0.166	1.34	1.10
169689	6902	0.98 <sup>c</sup>	4900 <sup>c</sup>	14	≥0.7	0.238	1.78	1.42
170659	...	1.61	3748	≤4	≤-1.0	...	...	...
175492	7133	0.93 <sup>b</sup>	4984	12	≥0.7	0.246	1.53	1.23
181154	...	1.14	4587	≤4	≤-0.3	0.184	1.33	1.08
190299	7667	1.24	4415	≤4	≤-0.5	0.181	1.37	1.11
202320	8127	1.10	4658	≤4	≤-0.2	0.183	1.44	1.18
204082	...	1.38 <sup>b</sup>	4176	≤4	≤-0.8	0.166	1.30	1.08
204540	...	1.19	4500	7	-0.1	0.181	1.35	1.09
212320	8530	0.95	4943	6	0.4	0.176	1.40	1.15
218527	8807	0.88	5090	≤4	≤0.4	0.218	1.44	1.14
219025	...	1.11	4640	456	3.3	...	...	...
221776	8950	1.51	3964	≤4	≤-1.0	0.183	1.41	1.15
233517	...	1.16 <sup>b</sup>	...	...	...	0.218	0.174	1.29

<sup>a</sup> ( $B-V$ )<sub>0</sub> = ( $B-V$ ) -  $A_V/3$ , where  $A_V = 1 \text{ mag kpc}^{-1}$ .

<sup>b</sup> ( $B-V$ )<sub>0</sub> from spectral type-( $B-V$ ) relation of Gray 1992.

<sup>c</sup> ( $B-V$ )<sub>0</sub> and  $T_{\text{eff}}$  assumed from Griffin et al. 1995.

width resulting from the sometimes broad H $\alpha$  wings.

Table 3 presents the results of the H $\alpha$  measurements for the 39 KPNO program stars plus HDE 233517 and HD 219025. Columns (1) and (2) give the HD and HR numbers, respectively. Column (3) lists the computed ( $B-V$ )<sub>0</sub> of each star. Columns (4), (5), and (6) were discussed previously in § 5. Columns (7)–(9) give the H $\alpha$  residual intensity, the H $\alpha$  FWHD, and the H $\alpha$  core equivalent width, respectively. Table 4 lists the same H $\alpha$  measurements for 10 bright G and K giants that were used as spectral type or radial velocity standards. The latter stars are normal giants with no infrared excesses.

The H $\alpha$  residual intensity, the H $\alpha$  FWHD, and the H $\alpha$  core equivalent width of the two groups are plotted versus their ( $B-V$ )<sub>0</sub> colors in Figures 2a, 2b, and 2c, respectively. Also plotted in the three figures are the values for HDE 233517. As noted by Eaton (1995) in his extensive study of the H $\alpha$  line in cool giants, late-type giants show only slight changes in H $\alpha$  shape and equivalent width with spectral type. While there are no major systematic differences between the vast majority of the infrared-excess giants and

the normal giants plotted in Figures 2a, 2b, and 2c, the position of HDE 233517 clearly stands out in all three plots. In addition, several of the infrared-excess giants stand out in two of the three plots. The reasons for their positions in the plots are discussed below.

TABLE 4  
H $\alpha$  OF NORMAL GIANTS

HR	Name	$B-V$ (mag)	( $B-V$ ) <sub>0</sub> <sup>a</sup> (mag)	$R_c$	FWHD (Å)	EW <sub>c</sub> (Å)
617	$\alpha$ Ari	1.15	1.14	0.183	1.34	1.08
1283	$\omega^1$ Tau	1.07	1.04	0.189	1.31	1.08
2985	$\kappa$ Gem	0.93	0.92	0.177	1.34	1.13
2990	$\beta$ Gem	1.00	1.00	0.187	1.31	1.06
3145	...	1.25	1.22	0.172	1.35	1.10
4695	16 Vir	1.16	1.13	0.183	1.39	1.12
4954	41 Com	1.48	1.45	0.185	1.38	1.11
6148	$\beta$ Her	0.94	0.92	0.182	1.40	1.18
6603	$\beta$ Oph	1.16	1.15	0.196	1.29	1.04
8551	35 Peg	1.05	1.03	0.186	1.29	1.07

<sup>a</sup> ( $B-V$ )<sub>0</sub> = ( $B-V$ ) -  $A_V/3$ , where  $A_V = 1 \text{ mag kpc}^{-1}$ .

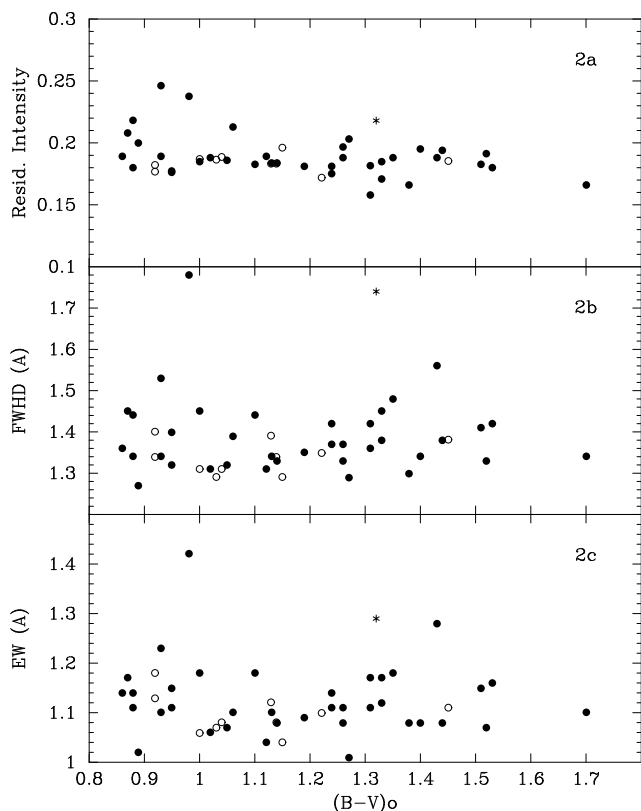


FIG. 2.—Variation of (a) residual intensity, (b) FWHD, and (c) equivalent width for  $H\alpha$  with  $(B-V)_0$ . Filled circles, IR-excess giants; open circles, normal giants; asterisk, HDE 233517.

On the blue side of the  $(B-V)_0$  axis, the two stars with the most discrepant  $H\alpha$  results are HR 6902 and HR 7133. Those two, however, are composite-spectrum binaries whose  $H\alpha$  measurements are anomalous because of the presence of a B- or A-type companion in combination with the late-type giant. Two other stars on the blue side, HR 4249 and HR 8807, are also of interest. Their  $H\alpha$  properties are similar to each other but less anomalous than HR 6902 or HR 7133. HR 4249 is a spectroscopic binary with an orbital period of 1166 days (Griffin 1980), but its secondary so far has not been seen. The new velocities listed in Table 2 show that HR 8807 is also a spectroscopic binary. In one spectrum, weak secondary lines, likely from an F star, are visible. Thus, HR 8807, like HR 7133 and HR 6902, is a composite-spectrum binary. Toward the red end of the  $(B-V)_0$  axis, HR 6078 stands out. However, while its  $H\alpha$  equivalent width and FWHD appear anomalous when compared with giant stars, those values are very similar to the mean values that Eaton (1995) found for bright giants. The *Hipparcos* parallax and an assumed reddening of 0.26 mag result in  $M_V = -1.44$  mag, indicating that it is indeed more luminous than a typical giant. In conclusion, none of the 39 giants have  $H\alpha$  properties similar to those of HDE 233517.

#### 7. HD 219025

Houk & Cowley (1975) classified HD 219025 as K2 IIIp and commented that the Ca II H and K cores are in emission. Despite the giant identification, Whitelock et al. (1995) preferred a pre-main-sequence interpretation based on its

large lithium abundance (Randich et al. 1993) and infrared variability. Fekel et al. (1996) argued that this infrared-excess star is indeed a post-main-sequence giant with optical properties similar to HDE 233517. The *Hipparcos* parallax of 0'00325 confirms that the star is a giant with  $M_V = -0.1$  and a radius of  $18.2 R_\odot$ .

The absorption lines show significant line broadening consistent with the  $v \sin i$  value of  $20 \text{ km s}^{-1}$  found by Randich et al. (1993). From the MJUO spectra we estimate a value of  $25 \text{ km s}^{-1}$ .

Our value of 3.3 for the log lithium abundance of HD 219025 (Table 3) has an estimated uncertainty of 0.6 dex. Despite this large uncertainty, this giant is clearly lithium-rich, as first indicated by Randich et al. (1993).

Of the observed infrared-excess giants, HD 219025 is clearly the most similar to HDE 233517. It is unfortunate that we were unable to obtain a good spectrum of its  $H\alpha$  region for comparison.

#### 8. INFRARED EXCESSES

Fekel & Balachandran (1993) obtained spectroscopic observations of a group of rapidly rotating, chromospherically active, single giants. Additional giants were identified by Fekel & Balachandran (1994) and Fekel et al. (1996). Besides the rapid rotation, many of those giants have unexpectedly high lithium abundances. Fekel & Balachandran (1993) argued that such rapid rotation is a brief evolutionary stage in first-ascent giants. They suggested a scenario in which the surface convection zone reaches the rapidly rotating core as a star begins its first ascent of the giant branch and dredges up to the surface high angular momentum material and freshly synthesized lithium. They argued that while such a state would be short-lived, the development and decay of rapid rotation would not necessarily have the same timescale as the enhancement and depletion of the surface lithium abundance. They also noted that the lithium enrichment might well occur over a limited mass range.

As discussed by Fekel et al. (1996), the chromospherically active giants HDE 233517 and HD 219025 provide a connection between the above scenario and one developed by de la Reza et al. (1996), which links infrared excesses and the large lithium abundances possessed by a small fraction of late-type giants. In their scenario, every star having a mass of  $1-2.5 M_\odot$  becomes lithium-rich while a K giant, and the mechanism responsible for the enhancement also creates a mass-loss event, resulting in an observed infrared excess. As such a circumstellar shell expands, cools, and dissipates, its infrared fluxes change, changing the position of the star in an infrared color-color diagram.

Assuming various starting parameters, de la Reza et al. (1996) plotted evolutionary tracks for detached circumstellar shells in an infrared color-color diagram and compared the results with a number of observed K giants. Their evolutionary tracks begin in the lower left-hand corner of the color-color plot, and the stars move counterclockwise around the diagram. The most extended tracks in the color-color plot are followed by stars having the largest mass-loss rates. Stars with the largest infrared color excesses and presumably large lithium abundances appear to populate the right-hand side of the diagram. De la Reza et al. (1997) expanded the observed sample of infrared excess giants, increasing the number of lithium-rich giants as well as including some giants from Zuckerman et al. (1995).



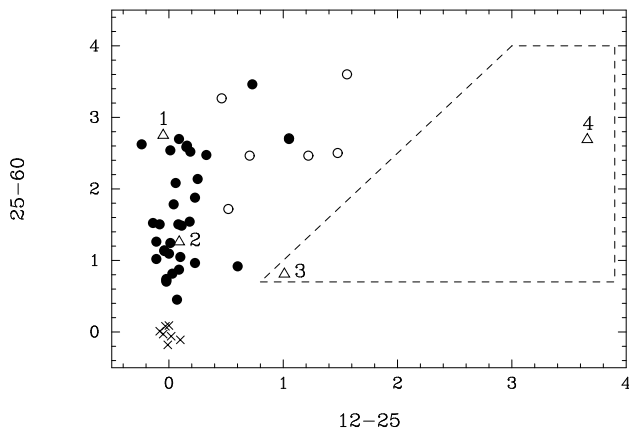


FIG. 3.—*IRAS* color-color diagram. Filled circles, IR-excess giants with no flux upper limits; open circles, IR-excess giants with one flux upper limit; crosses, normal giants; open triangles, chromospherically active giants (1 = HD 9746, 2 = HD 31993, 3 = HD 219025, 4 = HDE 233517). Dashed line, region where most giants are lithium rich.

There is no standard method to convert *IRAS* fluxes of various bandpasses into colors. Thus, a variety of “color” formulae have appeared in the literature (e.g., van der Veen & Habing 1988; Zijlstra et al. 1992; Hickman, Sloan, & Canerna 1995). From the 12, 25, and 60  $\mu\text{m}$  fluxes listed by Zuckerman et al. (1995), the *IRAS* colors of the present sample were computed with the formulae of Hickman et al. (1995). A color-color plot (Fig. 3) similar to that of de la Reza et al. (1997) is shown for the 39 giants. Also included in the figure are giants without infrared excesses (Table 4), as well as HDE 233517 and HD 219025, plus two other lithium-rich, chromospherically active giants, HD 9746 and HD 31993. Infrared fluxes for the latter two groups were taken from the SIMBAD database. The region where most infrared-excess giants are lithium-rich (de la Reza et al. 1997) has been outlined by a dashed line.

The normal giants, having no infrared excesses, are tightly grouped at the lower left-hand corner of the color-color plot. The vast majority of the program stars, are aligned vertically along the left axis. In terms of the scenario of de la Reza et al. (1996), such stars are nearing the end of their circumstellar-shell evolution. Seven of the 39 giants have large (25–60) excesses and moderate (12–25) excesses. For six of the seven, one flux, usually that at 25  $\mu\text{m}$ , is an upper limit. Knowledge of the true value of this flux would shift the points down and to the right in the diagram. Although those seven stars stand out in the color-color diagram, only one of them, HD 21078, is apparently lithium-rich.

HDE 233517, with its very large infrared excesses, appears alone on the right-hand side of the diagram. According to de la Reza et al. (1997), this region should be sparsely populated since the circumstellar-shell evolution in this area of the plot is extremely fast.

The position of HD 219025 in the infrared color-color diagram (Fig. 3) is not as extreme as that of HDE 233517 but does suggest a recent low mass loss rate event, according to the scenario of de la Reza et al. (1996, 1997). On the other hand, none of the 39 KPNO infrared-excess giants have properties similar to HDE 233517. It is possible, however, that some similar stars may exist. De la Reza et al. (1997) added 20 new lithium-rich giants to their infrared color-color diagram. If the scenarios of Fekel & Balachandran (1993) and de la Reza et al. (1996) are indeed linked, many of those newly identified lithium-rich giants should be rapidly rotating, have Ca II H and K emission, and might well have peculiar H $\alpha$  profiles similar to HDE 233517.

## 9. INDIVIDUAL STARS

**HD 21078.**—The *Hipparcos* parallax of this star (Table 1) indicates that it is a subgiant. Spectroscopic observations show that it has a variable velocity, and observations are continuing to determine its orbit.

**HR 1360.**—Six Mount Wilson Observatory radial velocities have a range of 12 km s<sup>-1</sup> (Abt 1970). The three KPNO velocities (Table 2) confirm the velocity variation.

**HR 6078.**—Castilho et al. (1995) identified this star as a moderately lithium-rich K giant. From an abundance analysis based on their high-resolution spectra, they found it to be slightly metal-poor with [Fe/H] =  $-0.3 \pm 0.15$ . With  $T_{\text{eff}} = 4000$  K they found  $\log \epsilon(\text{Li}) = 1.6$ . Three Mount Wilson Observatory velocities have a range of 26 km s<sup>-1</sup> (Abt 1973). Two are  $-50$  km s<sup>-1</sup> while one is  $-24$  km s<sup>-1</sup>. The KPNO velocities (Table 2) are similar to the latter velocity. Thus, this star is probably a binary.

**HD 183526.**—Houk’s (1982) classification of this star is K3 III:, but that classification is a typographical error. The star was on our initial list of program stars and was eliminated from the final list when two observations of the lithium region showed an M giant spectrum. N. Houk’s (1998, private communication) corrected classification is M3 III:.

**HR 8807.**—The six velocities listed in Table 2 show a range of 30 km s<sup>-1</sup>. In one spectrum, weak secondary lines, likely from an F star, are visible. The binary nature of HR 8807 was also discovered from *Hipparcos* observations (ESA 1997) and CORAVEL observations (J. R. de Medeiros 1998, private communication). The *Hipparcos* satellite observations result in an orbital period of 781 days (ESA 1997). Spectroscopic observations are continuing.

**HD 219025.**—The two velocities listed in Table 2 show no velocity variation, suggesting that this rapidly rotating giant may be single, but are only a day apart.

We thank J. R. de Medeiros for providing data in advance of publication. The helpful comments of the referee are appreciated. This research has been supported in part by NASA grant NCC 5-228 plus NSF grants HRD 95-50561 and HRD 97-06268 to Tennessee State University.

## REFERENCES

- Abt, H. A. 1970, *ApJS*, 19, 387  
 ———, 1973, *ApJS*, 26, 365  
 Bopp, B. W., Dempsey, R. C., & Maniak, S. 1988, *ApJS*, 68, 803  
 Brown, J., Sneden, C., Lambert, D. L., & Dutchover, E. 1989, *ApJS*, 71, 293  
 Castilho, B. V., Barbuy, B., & Gregorio-Hetem, J. 1995, *A&A*, 297, 503  
 Castilho, B. V., Gregorio-Hetem, J., Spite, F., Spite, M., & Barbuy, B. 1998, *A&AS*, 127, 139  
 de la Reza, R., Drake, N. A., & da Silva, L. 1996, *ApJ*, 456, L115  
 de la Reza, R., Drake, N. A., da Silva, L., Torres, C. A. O., & Martin, E. L. 1997, *ApJ*, 482, L77  
 de Medeiros, J. R., da Rocha, C., & Mayor, M. 1996, *A&A*, 314, 499  
 de Medeiros, J. R., & Mayor, M. 1990, in *ASP Conf. Ser. 9, Cool Stars, Stellar Systems, and the Sun: Sixth Cambridge Workshop*, ed. G. Wallerstein (San Francisco: ASP), 404  
 de Medeiros, J. R., Melo, C. H. F., & Mayor, M. 1996, *A&A*, 309, 465  
 Eaton, J. A. 1995, *AJ*, 109, 1797

- ESA. 1997, *The Hipparcos and Tycho Catalogues* (ESA SP-1200) (Noordwijk: ESA)
- Fekel, F. C. 1997, *PASP*, 109, 514
- Fekel, F. C., & Balachandran, S. 1993, *ApJ*, 403, 708
- . 1994, in *ASP Conf. Ser. 64, Cool Stars, Stellar Systems, and the Sun: Eighth Cambridge Workshop*, ed. J.-P. Caillault (San Francisco: ASP), 279
- Fekel, F. C., Webb, R. A., White, R. J., & Zuckerman, B. 1996, *ApJ*, 462, L95
- Fitzpatrick, M. J. 1993, in *ASP Conf. Ser. 52, Astronomical Data Analysis Software and Systems II*, ed. R. J. Hanisch, R. V. J. Brissenden, & J. Barnes (San Francisco: ASP), 472
- Flower, P. J. 1996, *ApJ*, 469, 355
- Gray, D. F. 1989, *ApJ*, 347, 1021
- . 1992, *The Observation and Analysis of Stellar Photospheres* (2d ed.; Cambridge: Cambridge Univ. Press), 430
- Gregorio-Hetem, J., Castilho, B. V., & Barbuy, B. 1993, *A&A*, 268, L25
- Gregorio-Hetem, J., Lépine, J. R. D., Quast, G. R., Torres, C. A. O., & de la Reza, R. 1992, *AJ*, 103, 549
- Griffin, R. E. M., Marshall, K. P., Griffin, R. F., & Schröder, K.-P. 1995, *A&A*, 301, 217
- Griffin, R. F. 1980, *Observatory*, 100, 161
- Hearnshaw, J. B. 1977, *Proc. Astron. Soc. Australia*, 3, 102
- . 1978, *S&T*, 56, 6
- Hickman, M. A., Sloan, G. C., & Canterna, R. 1995, *AJ*, 110, 2910
- Houk, N. 1982, *Michigan Catalogue of Two-dimensional Spectral Types for the HD Stars, Vol. 3* (Ann Arbor: Univ. Michigan Dept. Astron.)
- Houk, N., & Cowley, A. P. 1975, *Michigan Catalogue of Two-dimensional Spectral Types for the HD Stars, Vol. 1* (Ann Arbor: Univ. Michigan Dept. Astron.)
- Houk, N., & Smith-Moore, M. 1988, *Michigan Catalogue of Two-dimensional Spectral Types for the HD Stars, Vol. 4* (Ann Arbor: Univ. Michigan Dept. Astron.)
- Iben, I. 1967a, *ApJ*, 147, 624
- . 1967b, *ApJ*, 147, 650
- Keenan, P. C., & McNeil, R. C. 1989, *ApJS*, 71, 245
- Nankivell, G. R., & Rumsey, N. J. 1986, in *IAU Symp. 118, Instrumentation and Research Programmes for Small Telescopes*, ed. J. B. Hearnshaw & P. L. Cottrell (Dordrecht: Reidel), 101
- Pallavicini, R., Cerruti-Sola, M., & Duncan, D. K. 1987, *A&A*, 174, 116
- Pallavicini, R., Randich, S., & Giampapa, M. S. 1992, *A&A*, 253, 185
- Plets, H., Waelkens, C., Oudmaijer, R. D., & Waters, L. B. F. M. 1997, *A&A*, 323, 513
- Randich, S., Gratton, R., & Pallavicini, R. 1993, *A&A*, 273, 194
- Roman, N. G. 1952, *ApJ*, 116, 122
- Scarfe, C. D., Batten, A. H., & Fletcher, J. M. 1990, *Publ. Dominion Astrophys. Obs. Victoria*, 18, 21
- Skinner, C. J., Sylvester, R. J., Graham, J. R., Barlow, M. J., Meixner, M., Keto, E., Arens, J. F., & Jernigan, J. G. 1995, *ApJ*, 444, 861
- Soderblom, D. R., Jones, B. F., Balachandran, S., Stauffer, J. R., Duncan, D., Fedele, S. B., & Hudon, J. D. 1993, *AJ*, 106, 1059
- Strassmeier, K. G., & Fekel, F. C. 1990, *A&A*, 230, 389
- Strassmeier, K. G., Fekel, F. C., Bopp, B. W., Dempsey, R. C., & Henry, G. W. 1990, *ApJS*, 72, 191
- van der Veen, W. E. C. J., & Habing, H. J. 1988, *A&A*, 194, 125
- Walker, H. J., & Wolstencroft, R. D. 1988, *PASP*, 100, 1509
- Whitelock, P., Menzies, J., Feast, M., Catchpole, R., Marang, F., & Carter, B. 1995, *MNRAS*, 276, 219
- Zijlstra, A. A., Loup, C., Waters, L. B. F. M., & de Jong, T. 1992, *A&A*, 265, L5
- Zuckerman, B., Kim, S. S., & Liu, T. 1995, *ApJ*, 446, L79